Inflammation, Vol. 42, No. 1, February 2019 (© 2018)
DOI: 10.1007/s10753-018-0869-5

ORIGINAL ARTICLE

Induced Expression of Endogenous CXCR4 in iPSCs by Targeted CpG Demethylation Enhances Cell Migration Toward the Ligand CXCL12

Can Jiang,[1] Jun Guo,[1,3] Huaiyan Cheng,[2] and Ying-Hong Feng[2]

Abstract— Poor homing of cells after transplantation is an unresolved common issue in cardiac cell therapies. To enhance stem cell homing, the ligand CXC motif chemokine 12 (CXCL12) and its specific receptor CXC receptor type 4 (CXCR4) have been employed as a system in this study to show that induced expression of the endogenous CXCR4 gene in mouse-induced pluripotent stem cells (iPSCs) improved the cell migration. Loci-specific epigenome editing in the form of CpG demethylation at CXCR4 promoter region of the mouse iPSCs was accomplished with CXCR4b-TAL-Tet1c, chimeric fusion proteins of the catalytic domain of ten-eleven translocation 1 (TET1) to the C-terminal end of the DNA binding domains of predesigned synthetic transcription activator-like effectors (TALEs) that recognize specific DNA sequences within the mouse CXCR4 promoter region. Infection of the mouse iPSCs with the engineered CXCR4b-TAL-Tet1c in the form of lentiviral particles induced the loci-specific CpG demethylation and subsequent activation of CXCR4 expression in mouse iPSCs. As expected, the CXCR4-overexpressing iPSCs exhibited 3.9-fold greater migration than the control iPSCs did without alteration of the stemness and activated phosphorylation of AKT significantly. These results set a sound foundation for subsequent *in vivo* iPSCs transplantation studies in rodent models of acute myocardial infarction and heart failure. We show that TALEs can enhance the expression of CXCR4 by CpG methylation, and may retain the stemness. Migration of iPSCs activated by CXCL12 is associated with significant phosphorylation of AKT, not ERK1/2.

KEY WORDS: IPSCs (induced pluripotent stem cells); TALEs (transcription activator-like effectors); CXCR4; CpG methylation; epigenome editing.

Coronary heart disease (CHD) remains a leading cause of mortality worldwide. It often manifests as sudden cardiac death, devastating acute myocardial infarction, and heart failure. Increasing evidence indicates that stem or progenitor cells recruited from circulation or directly injected to the site of ischemic myocardium could participate in regeneration of the heart tissue and improve the cardiac function [1, 2].

Induced pluripotent stem cells (iPSCs) generated from terminally differentiated somatic cells upon ectopic overexpression of transcription factors Oct4,

Can Jiang and Jun Guo contributed equally to this work.

Electronic supplementary material The online version of this article (https://doi.org/10.1007/s10753-018-0869-5) contains supplementary material, which is available to authorized users.

[1] Department of Cardiology, The First Affiliated Hospital of Jinan University, Guangzhou, 510630, People's Republic of China
[2] Department of Pharmacology & Molecular Therapeutics, Uniformed Services University of the Health Sciences, Bethesda, MD 20814, USA
[3] To whom correspondence should be addressed at Department of Cardiology, The First Affiliated Hospital of Jinan University, Guangzhou, 510630, People's Republic of China. E-mail: jndxgj@163.com

Sox2, Lin28, Nanog, Klf4, and c-Myc represent an attractive resource for cardiac stem cell therapy [3]. In addition to many advantages such as unlimited self-renewal and pluripotency, iPSCs can be improved with genome editing or epigenome editing technologies for therapeutic research. Lentiviral particles are some of the efficient gene delivery vehicles to overexpress ectopic transgenes.

Genome-editing tools including engineered zinc-finger nucleases (ZFN), transcription activator-like effectors (TALEs), and CRISPR/Cas9 have gained high attention over time as attractive biotechnology tools since they all recognize specific DNA sequences as needed [4–6]. CRISPR/Cas9 system needs an additional partner gRNA to target the selected DNA sequence [7], which creates more complexity and difficulty to certain applications. TALEs are usually hard to synthesize, but could be more efficient than CRISPR/Cas9 in genome editing [8], and TALEs also showed less nuclease-associated cytotoxicity when compared to ZFN [9]. TALEs armed with catalytic domains of DNA CpG demethylase and methyltransferase have been successfully utilized to reactivate expression of several endogenous genes [10, 11].

The C-X-C motif chemokine 12 (CXCL12), also known as stromal cell-derived factor 1 (SDF1), is the specific ligand of C-X-C chemokine receptor type 4 (CXCR4). It is transcriptionally upregulated and released to the local peripheral blood immediately after myocardial infarction (MI). As a chemoattractant, CXCL12 plays an important role in stem cell migration toward the infarct area. It has been shown that interactions between CXCL12 and CXCR4 in the injured tissues regulate the recruitment and retention of progenitor cells, bone marrow mesenchymal stem cells, and bone marrow mononuclear cells [12–14]. The CXCL12/CXCR4-mediated recruitment of stem cells to the ischemic heart has been shown to improve vessel growth and myocardial function in preclinical models [15].

In this study, TALEs technology has been utilized to activate expression of endogenous CXCR4 in mouse iPSCs by loci-specific epigenomic CpG demethylation of CXCR4 promoter region with infection lentiviral particles containing CXCR4b-TAL-Tet1c. We demonstrated that expression of CXCR4 can be effectively activated, and the overexpressed CXCR4 robustly enhances migration of the iPSCs toward CXCL12.

METHODS

Characterization and Expansion of iPSCs

Briefly, mouse iPSCs passed to the 13th generation were kindly provided by Stem Cell Bank, Chinese Academy of Sciences [16]. 1.0×10^6cells/cm^2 iPSCs were seeded into a T-25 tissue cell culture flasks coated with a layer of mitotically inactivated mouse embryonic fibroblasts (MEFs) by mitomycin C-treatment in dulbecco's Modified Eagle Medium and Nutrient Mixture F-12 (DMEM/F-12, Gibco, NY, USA) containing 15% fetal bovine serum (FBS, Gibco, NY, USA), 1% (*v*/*v*) nonessential amino acids (NEAA, Gibco, NY, USA), 1% (*v*/*v*) nucleosides (Millipore, Billerica, MA), 500 units/ml leukemia inhibitory factor (LIF, Millipore, Billerica, MA), 0.1 mM β-Mercaptoethanol (Invitrogen, NY, USA), and1% (*v*/*v*) penicillin and streptomycin (pen/strep, Gibco, NY, USA) at an incubator set 37 °C under 5% CO_2 environment. At 80–90% confluence, iPSCs were passaged using 0.25% Trypsin/EDTA (Gibco, NY, USA) every 2–3 days.

CXCR4 Reporter Construction and *in vitro* CpG Methylation

Based on mouse, rat, and human CXCR4 core promoters predicted with Proscan (http://www-bimas.cit.nih.gov/molbio/proscan/), a mouse CXCR4 gene promoter region (− 321/+ 105) was amplified from mouse genomic DNA using specific primers (Forward: TGCAGTAA CACACACTTGCTTGG, and Reverse: GATGCAAG TGGACTTACTTCCATGG). The PCR products were cloned into the CpG-free pCpGL vector with HindIII and NcoI sites (a gift from Michael Rehli). The reporter was treated with and without non-specific CpG methyltransferase M.SssI (http://NEB.com) according to the manufacturer's instructions, and the methylation was confirmed by Hae II digestion (http://NEB.com). The insert fragments of the reporter described above were verified by DNA sequencing.

Luciferase Reporter Activity Assay

Transfection of plasmids in specified cells was carried out using Lipofectamine 2000 (Invitrogen) according to the manufacturer's instructions. For locus-specific CpG demethylation of the CXCR4b-pCpGL reporter, subsequent transient co-transfection of the reporter together with CXCR4b-TAL-Tet1c plasmid in phCMV1/FRT vector at DNA ratio of 1:4 was performed with HEK293 cells and

COS1 cells. About 24 h after the transfection, the luciferase activities were assayed, using a Dual Glo luciferase kit (Promega), in specified cells that were co-transfected with dual luciferase reporters alone or together with CXCR4-TAL-Tet1c plasmid following the manufacturer's instructions. All data were normalized as relative firefly luciferase light/renilla units.

Plasmid Construction, Lentiviral Production, and Titration

The CXCR4b-TAL-Tet1c synthetic fusion gene was constructed as shown in supplemental Fig. S1 in Dr. Feng's laboratory, Uniformed Services University of the Health Sciences, Bethesda, Maryland, USA [11]. Briefly, the DNA binding domains of the TALEs targeting mouse CXCR4 promoter regions were synthesized by an in-house assembly technology of sequential ligation. The assembled DNA binding domains consisting of 22–24 repeats were fused to the catalytic domain of Tet1 with AscI site. The complete CXCR4b-TAL-Tet1c that contains a NLS at either end of the DNA binding domain was fully sequenced and subcloned into the in-house phCMV1/FRT vector, lentiviral vector pCDH-EF1-MCS-Puro, and pCDH-EF1-MCS-T2A-Puro-GFP (System Biosciences, Mountain View, CA, USA), respectively.

For lentiviral particle preparation, 293FT cells (Cyagen Biosciences Inc.) in the logarithmic growth phase were incubated overnight in an 100-mm dish at a density of 5×10^6 cells/dish at 37 °C and 5% CO_2. The CXCR4b-TAL-Tet1c containing plasmid in pCDH-EF1-MCS-Puro and pCDH-EF1-MCS-T2A-Puro-GFP vector was co-transfected with the lentiviral packaging plasmid into the 293FT cells using lipofectamine 2000 transfection reagent (Invitrogen, NY, USA) in a dropwise manner. About 72 h after transfection, the culture supernatant containing lentiviral particles was collected and concentrated, and then the virus was subpacked. The sample was then stored at − 80 °C for future determination of the biological virus titer. The virus titers were preliminarily determined according to their fluorescent expression.

Transfection

The iPSCs in the logarithmic growth phase were detached from feeder cells using 0.05% trypsin for 3 min, washed once with DMEM/F12, and clumps were broken up by pipetting. 1×10^5 cells were seeded in a 6-well plate, then infected with lentiviral particles expressing CXCR4b-TAL-Tet1c and/or GFP separated by a T2A motif in the presence of polybrene (5 μg/ml) at a multiplicity of infection of 10. Twenty-four hours later, fresh iPSCs medium was added, and transduced cells were further cultivated as described above. The iPSCs were analyzed after 2–3 days.

Morphological Appearance

To observe the induced expression of CXCR4 in iPSCs, embryoid bodies were seeded on gelatin-coated coverslip in a 6-well plate for 2 days. The iPSCs were washed three times with 0.01% PBS and fixed in 4% paraformaldehyde for 20 min at room temperature. After washing, the cells were blocked in 10% BSA for 30 min at room temperature, then incubated with primary antibodies against CXCR4 (Abcam, MA, USA 1:200) at 4 °C overnight. Subsequently, the cells were incubated in the fluorophore-conjugated secondary antibodies that were conjugated to APC (Abcam, MA, USA 1:1000), respectively, for 30 min. Ultimately cells were stained with 4,6-diamidino-2-phenylindole (DAPI) (Sigma, MO, USA) and observed under a fluorescence microscope.

Real-Time PCR

Total RNA was extracted using TRIzol reagent (Invitrogen, NA, USA) according to the manufacturer's instructions. Reverse transcription-polymerase chain reaction was performed with SYBR FAST qPCR kit Master Mix (2×) Universal (KAPA). The primer sequences used were listed as follows: CXCR4 forward:5′-CTCTGAGGCGTTTG GTGCTC-3′, reverse: 5′-CGGAAGCAGGGTTC CTTGTT-3′; c-Myc forward: 5′-GGAAACGACGAGAA CAGTTG-3′; c-Myc reverse:5′-GCCAAGGTTGTGAG GTTAGG-3′; Oct4 forward:5′-AGGATGTGGTTCGA GTATGGTT-3′, reverse:5′-AAGGGACTGAGTAG AGTGTGGTG-3′; GAPDH forward:5′-AGGAGCGA-GACCCCACTAACA-3′, reverse:5′-AGGG GGGCTAAGCAGTTGGT-3′. The fold changes of each target mRNA expression relative to GAPDH were calculated based on the threshold cycle. All experiments were repeated three times ($n = 3$).

Western Blot Analysis and Flow Cytometry (FCM)

RIPA lysis buffer (Thermo, MA, USA) was used to extract proteins from the iPSCs. These lysates were sonicated for 10 s and centrifuged at 12000 g for 15 min. The protein concentrations were determined using a BCA protein assay kit (Pierce). Equal amount of the lysates were loaded onto a 5% stacking and 10% resolving SDSPAGE gel. After electrophoresis, the proteins were transferred to

NC membranes by semidry transfer. After blocking for 1 h with 5% (*w*/*v*) bovine serum albumin dissolved in 0.1% TBS-T, membranes were incubated overnight at 4 °C with the following antibodies: mouse monoclonal anti-CXCR4, mouse monoclonal anti-AKT, mouse monoclonal anti-P-AKT, mouse monoclonal anti-ERK1/2, mouse monoclonal anti-p-ERK1/2, GAPDH (Abcam, MA, USA 1:100). After washing in 0.1% TBS-T, membranes were incubated with the horseradish peroxidase (HRP)-conjugated secondary antibodies (Abcam, MA, USA) for 1 h at room temperature. The samples on membranes were visualized by enhanced chemiluminescence (ECL) system (Invitrogen, NY, USA). The optical density was quantified using an image processing and analysis program (Scion image).

Non-tranfected and CXCR4-iPSCs were stained with APC-anti-CXCR4 monoclonal antibody and APC-goat-anti-mouse immunoglobulin G as isotype control (BD Biosciences) for 30 min at 4 °C. After the final wash (phosphate-buffered saline + 0.1% bovine serum salbumin), cells were characterized and quantified by flow cytometry (FACS-calibur, Becton-Dickinson, San Jose, CA, USA).

Cell Viability

An aliquot of cells (1×10^4) was washed in phosphate-buffered saline (PBS) twice, and then was seeded in 50 μl binding buffer and 5 μl 7-ADD for 15 min at 37 °C. After being added 450 μl binding buffer and 1 μl Annexin-PE, the cell suspension was again incubated for 20 min at 37 °C. It was analyzed on a FACS Caliber flow cytometer (Becton Dickinson, MA, USA). Fluorescence compensation on the flow cytometer was adjusted to minimize overlap of the 7-ADD and PE signals. A total of 10,000 events were acquired on five parameters for each sample and analyzed using CellQuest software.

Cell Migration Assays

To investigate whether overexpression of CXCR4 promotes migration of the iPSCs toward CXCL12, the iPSCs, CXCR4-iPSCs or Vector-iPSCs (5×10^4/well) were seeded in the upper chamber of the 24-well transwell (Corning Life Sciences, MA, USA) pretreatmented with or not CXCR4 specific blocker AMD3100 (10 μg/ml), ERK1/2 specific blocker PD98059 (20 μmol/L), AKT specific blocker LY294002 (20 μmol/L) 1 h, and the lower chamber were supplemented with or without CXCL12 (100 ng/ml). After incubation for 4 h, the cells were visualized under fluorescence microscope for staining with Trypan blue.

Bisulfite Sequencing PCR (BSP)

To verify the demethylation level of iPSCs, bisulfite sequencing PCR (BSP) was used. DNA was first modified by treatment with sodium bisulfite to convert all "C"s to uracil residues except for 5 mCs. Then the bisulfite-modified DNA were amplified by PCR, which performed in a RT-PCR instrument (MJ Mini personal Thermal Cycler, BIO-RAD) using PCR MasterMix (TOYOBO, shanghai, Chinese) under the touch-down program: 95 °C for 5 min, followed by 40 cycles of 95 °C for 15 s, 60 °C for 15 s, and 72 °C for 3 min. The BSP primers were designed with Proscan (http://www-bimas.cit.nih.gov/molbio/proscan/):BSP-CXCR4:183 bp, 15 CpG, BSP-CXCR4-F: 5′ GGTTTTGGATTTATATTGATTTAAAATATA, BSP-CXCR4-R: 5′CCAAACAACAAAATTAAAATTTCTAAC; BSP-C-Myc: 232 bp, 16 CpG, BSP-C-Myc-F: 5′ TTTGTTTTTTGAAGGGTAGGGT, BSP-C-Myc-R: 5′ AAAACAAAACCCCTCTCACTC; BSP-Oct4: 232 bp, 15 CpG, BSP-Oct4-F: 5′TGGTTGAGTGGGTT GTAAGGATAGGT; BSP-Oct4-R: 5′ACTCCAAC CCTACTAACCCATCACC; BSP-sox2:235 bp,23CG, BSP-sox2-F:5′ GGGGGATATAAAGGTTTTTTAG, BSP-sox2-R:5′ ACAAATTAATAAACAACCATCCA-TATAATA; BSP-klf4:231 bp,30CG, BSP-klf4-F:5′ GTTTTTTTAGTTTTTTATTTAGTAATT, BSP-klf4-R:5′ TTAAACTCAACAATATCCCCCAC; The PCR product was then subcloned into the pMD19-T vector, and at least eight clones from each group were ramdomly selected and sent for Sanger sequencing by Geneseed Biotech Co (guangzhou, China).

Statistical Analysis

The results were statistically analyzed using Sigmastat (SPSS) version 13.0. Two-tail unpaired Student's *t* test was used for comparisons between two means. One-way ANOVA was used for comparisons between three or more means. Statistical significance was considered if a *P* value is < 0.05 or 0.01.

RESULTS

Identification of CXCR4 Promoter and Evaluation of Promoter Sensitivity to CpG Methylation

To identify CXCR4 gene promoter, the proximal DNA sequences around TSS of human, rat, and mouse CXCR4 gene were analyzed, respectively, with online bioinformatics software Proscan (http://www-

bimas.cit.nih.gov/molbio/proscan/). The core promoters identified for rat and mouse CXCR4 genes are shown in Fig. S1. Then the promoter regions for mouse (−431/+105) and rat (−424/+103) were subcloned into a CpG-free pCpGL vector, respectively. Transient transfection of these promoter reporter plasmids in HEK293 cells and COS-1 cells induced robust luciferase expression. Approximate 130-fold increases for mouse and rat reporters and 400-fold increases for human reporter were observed over their empty vector controls, suggesting that conventional promoters as predicted are present within the promoter region. The rat and mouse share a highly conserved CXCR4 promoter region (Fig. S1), and their promoter reporter activities are indistinguishable when expressed in HEK293 cells of human origin and COS-1 cells of monkey origin. The threefold higher activity of human over mouse and rat reporters may simply suggest that the HEK293 and COS-1 cells are more favorable to human CXCR4 promoter.

CpG methylation sites that may regulate gene transcription are relatively rich within the mouse and rat CXCR4 promoter region as shown in Fig. S1. To evaluate if the promoters are sensitive to CpG methylation for regulation of CXCR4 transcription, the mouse and rat CXCR4 promoter reporters were pre-treated with non-specific CpG methyltransferase M.SSSI. Transient transfection of the M.SSSI-treated reporters in HEK293 cells and COS-1 cells almost completely abolished the luciferase activity observed for the untreated reporters, suggesting the CpG sites within the defined promoter region play an essential role in regulating CXCR4 expression. These findings laid foundation for manipulation of CXCR4 expression through loci-specific epigenome editing in disease models of mouse and rat.

Generation of Chimeric Demethylase for Loci-Specific Modification of CXCR4 Promoter

Based on a variety of criteria such as CpG distribution, distance from core promoter and TSS, preferred range of epigenomic modification, TALE binding requirements, and minimal homology to the target genome sequence (Fig. S2), two 22 bp sequences of CXCR4a (−134/−155, TGGACCCATACTGACTTAAAAC) and CXCR4b (+6/+27, TTCAATTTTGTTGCCTGGTGCA) within the mouse promoter region were selected for TALE targeting (Fig. S1 and S2). These targeting sequences do not fall into any endogenous CpG site. Query of these 22 bp sequences against the mouse genomes in Blastn search revealed no identical sequence stretches that are long enough to become a concern for off-target binding (Fig. S2). Then, genes encoding a TALE DNA-binding domain consisting of a truncated N-terminal with a nuclear localization signal (NLS), a middle tandem repeat domain, and a C-terminal linker were synthesized with an in-house technology of sequential ligation assembly. The genetic codons of the tandem repeats are optimized for mammalian cell expression. The RVD codes used for nucleotides A, C, G, and T were amino acids NI, HD, NN, and NG, respectively. The synthetic TALE DNA-binding domain was then fused to HA-Tag, transcription activation domain vp64, and the catalytic domain of CpG demethylase Tet1 (1418–2136aa) to generate CXCR4-TAL-HA, CXCR4-TAL-vp64, CXCR4-TAL-Tet1c, CXCR4-TAL-Tet1c-GFP, CXCR4-TAL-SetD2, CXCR4-TAL-KDM4d, and CXCR4-TAL-MLL in an in-house phCMV1/FRT vector, respectively (Fig. 1a). The SetD2, KDM4d, and MLL (KMT2A) proteins activate gene transcription with differential mechanisms.

To determine if the synthetic TALE DNA-binding domains recognize the corresponding targeting sequences and which one works better in CXCR4 promoter activation, the M.SSSI-treated and untreated CXCR4 reporters were co-transfected with the TALEs in HEK293 cells. The result suggested that CXCR4b worked much better than CXCR4a in activation of mouse CXCR4 reporter expression in the form of vp64, Tet1c, and Tet1c-GFP (data for CXCR4a not shown). The other domains of SetD2, KDM4d, and MLL did not result in significant transcriptional activation (data not shown). CXCR4b-TAL-vp64 successfully activated the both methylated and unmethylated reporters (Fig. 1b), suggesting that the TALE DNA-binding domain recognized the targeting sequence well at least in the form of plasmid reporter DNA. As shown in Fig. 1b for the methylated reporter, the cells co-transfected with CXCR4b-TAL-Tet1c plasmid showed almost 13-fold higher luciferase activity comparing to the CXCR4b-TAL-HA control although such increased activity accounted only for about 30% of the full activity of unmethylated reporter co-transfected with CXCR4b-TAL-HA control. This activation of CpG-methylated reporter suggests that Tet1c successfully induced CpG-demethylation of the promoter region as previously reported [11]. However, GFP directly fused to the C-terminal of Tet1c resulted in some degree of reduced activation (only sevenfold).

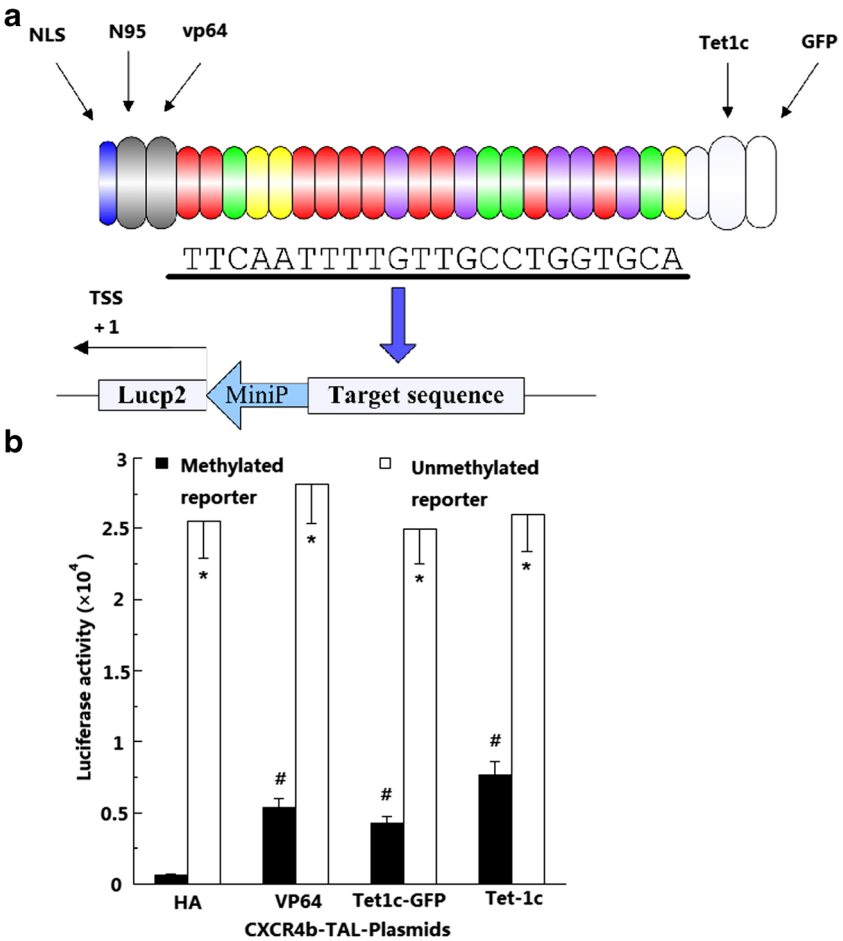

Fig. 1. Activation of CXCR4 reporter expression by locus-specific CpG demethylation. **a**. Illustration of the CXCR4b-TAL-effectors. The synthetic TALE DNA-binding domain, the 22 bp targeting sequence from mouse CXCR4 promoter region, nuclear localization signal (NLS), the truncated N-terminal domain (N95), the catalytic domain of Tet1 (Tet1c), the direct activation domain (vp64), and the other functional domain such as GFP are shown. The CXCR4 promoter structure (lower panel of **a**) is drawn on a non-proportional scale. TSS translation start site. **b** Luciferase activities altered by CXCR4b-TAL-effectors through locus-specific CpG demodification. Co-transfections with CXCR4b-TAL-effectors and the CpG-free CXCR4-pCpGL reporter pre-treated with and without M.SssI were performed in HEK293 and COS-1 cells. *$p < 0.001$ *vs* methylated reporters of the same group; #$p < 0.001$ *vs* methylated reporter of CXCR4b-AL-HA plasmid group.

Expression of CXCR4 and Cell Surface Distribution of CXCR4

To determine if transduction of the mouse iPSCs with CXCR4b-TAL-Tet1c lentiviral particles activates CXCR4 expression, RT-PCR Western blot and FCM were utilized. The mRNA levels in the Tet1c-transduced iPSCs significantly increased (1.8-fold, $p < 0.05$) comparing to that of the empty vector-transduced iPSCs (Fig. 2c). This significant increase at transcript level was translated into CXCR4 proteins with further amplification to about sixfold comparing to the control (Fig. 2d, e, $p < 0.05$). It has shown that the cell surface expression of CXCR4 significantly increased (Fig. 2f–g; 2.6-fold, $p < 0.05$).

To analyze if and how much the CXCR4 receptors that are forced to express in iPSCs, immunocytochemical staining was performed to visualize the receptor distribution. Results showed that CXCR4 receptors were obviously expressed on the iPSCs (Fig. 2a).

Effect of Expression of Endogenous CXCR4 on the ERK1/2 or AKT Signaling Pathway

Stem cells are small in size and the cell body is almost fully occupied by the nucleus. They also grow to form

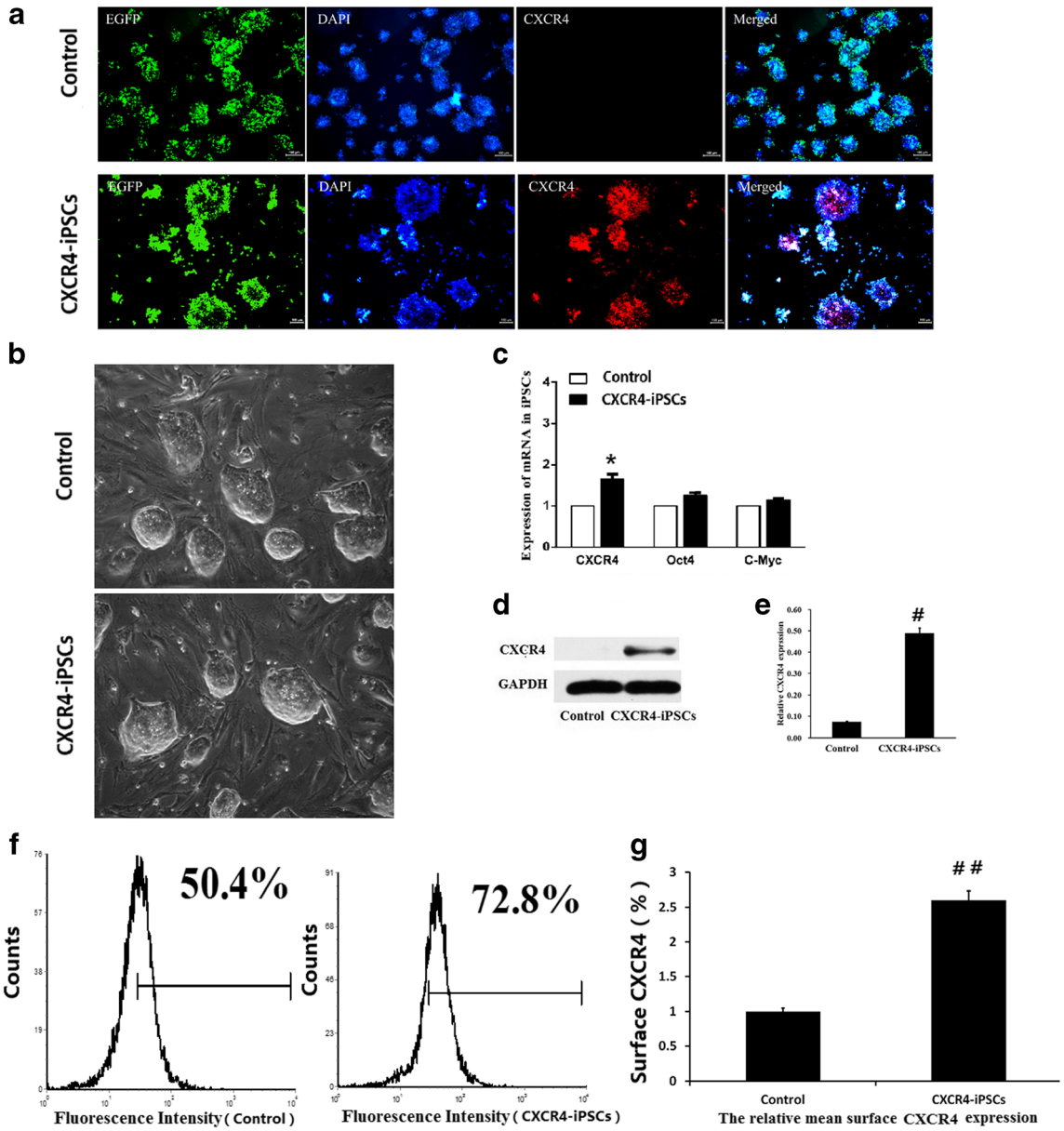

Fig. 2. Expression of endogenous CXCR4 and the effect on the infected iPSCs. **a** Representative image of distribution of expressed CXCR4 in iPSCs under fluorescence microscope. Detailed analysis of CXCR4 expression in cell spheres derived from an isolated single sphere of CXCR4-expressing iPSCs in serum-free medium. Scale bar 100 μm; **b** Representative images of the morphology of iPSCs after transfection (magnification × 100). Scale bar 100 μm. **c** The effect of expression of CXCR4 on stemness marker Oct4 and c-Myc mRNA. **d** The expression of CXCR4 after transfection. **e** Quantification and statistical analysis of the expression of experimental groups depicted in **d**. **f** The surface CXCR4 expression detected by FCM. **g** The statistical analysis of surface CXCR4 expression depicted in **f**. *Y*-axis shows the relative mean surface expression, and there are 2.6-fold increase in comparison to the control, which is taken as **f**. ($n = 3$, one-way ANOVA, $^{*}p < 0.05$ comparing to the control; $\#p < 0.01$ *versus* the control; $\#\#p < 0.01$ *versus* the control).

colonies. These properties make the stem cells difficult for visual analysis of a receptor distribution on the cell surface. Thus, functional signaling activation becomes necessary. In light of this, western blot analysis was performed with antibodies detecting phosphyorylated forms of the signaling molecules after ligand stimulation. The results showed that phosphorylation of extracellular signal-regulated kinases (Erk1/2) and protein kinase B (Akt) was significantly

elevated upon activation of CXCR4 by ligand CXCL12 ($p < 0.05$; Fig. 3). PI3K inhibitor (LY294002) could block phosphorylation of AKT, and phosphorylations of ERK1/2 were inhibited by MEK inhibitor (PD98059) in lower concentration ($p < 0.05$; Fig. 3). Figure 4 shows that AMD3100 inhibited AKT phosphorylation in a concentration dependent manner ($p < 0.05$), but no significant effect on ERK1/2 ($p > 0.05$). These results support that a significant portion of CXCR4 is indeed expressed on the iPSCs surface. The signaling strength initiated by the cell surface portion of the expressed CXCR4 receptor may be sufficient to produce needed chemotaxis action.

Apoptosis and Viability of Lentiviral-Infected iPSCs

Viral infection of stem cells may alter the cell viability. Figure 5 shows that infection of the iPSCs with the lentiviral particles indeed induced statistically significant apoptosis comparing to the uninfected control iPSCs ($p < 0.05$). Fortunately, no difference was found between Tet1c-infected iPSCs and the empty vector-infected iPSCs, suggesting ectopic expression of CXCR4b-TAL-Tet1c and forced expression of endogenous CXCR4 are not toxic to the cells tested in the experiment (Fig. 6).

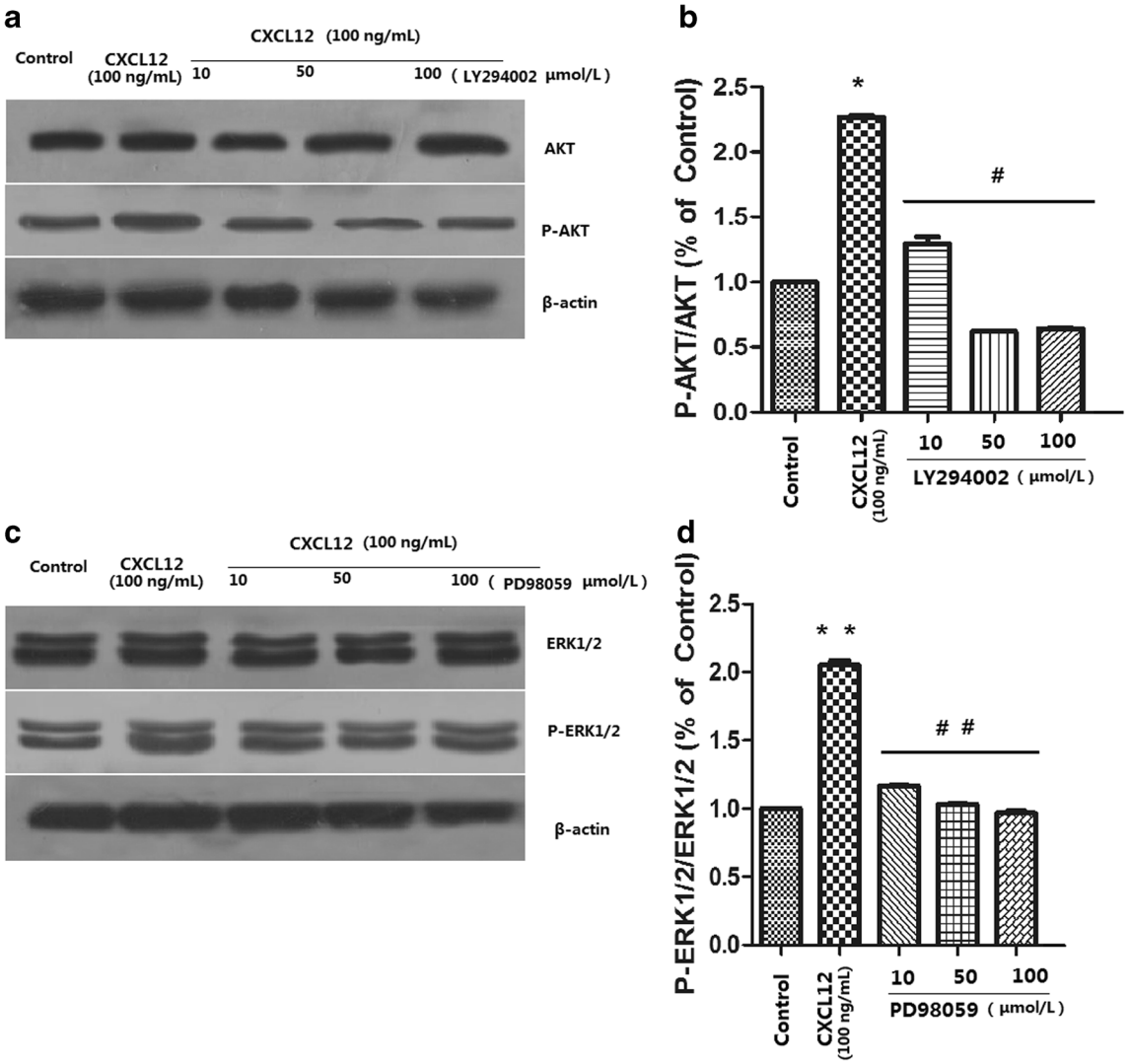

Fig. 3. CXCR4-mediated activation of AKT and ERK1/2 in iPSCs. β-actin was used as an internal control. ($n = 3$, one-way ANOVA, $*p < 0.05$ *versus* the control, $\#p < 0.01$ *versus* the CXCL12 group).

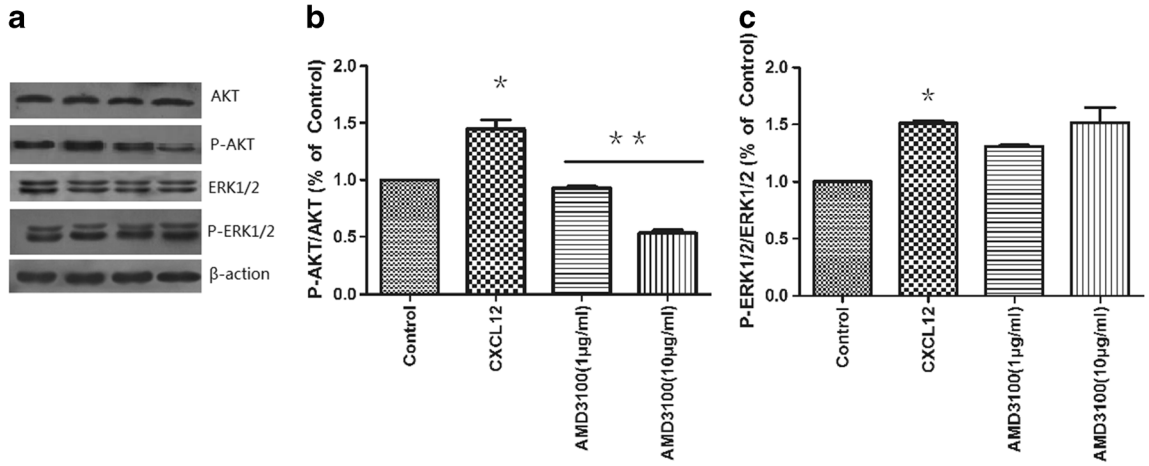

Fig. 4. The effection of AMD3100 on P-AKT and P-ERK1/2 in CXCR4-iPSCs after activation by CXCL12 β-actin was used as an internal control. ($n = 3$, one-way ANOVA, $*p < 0.05$ *versus* the control, $\#p < 0.01$ *versus* the CXCL12 group).

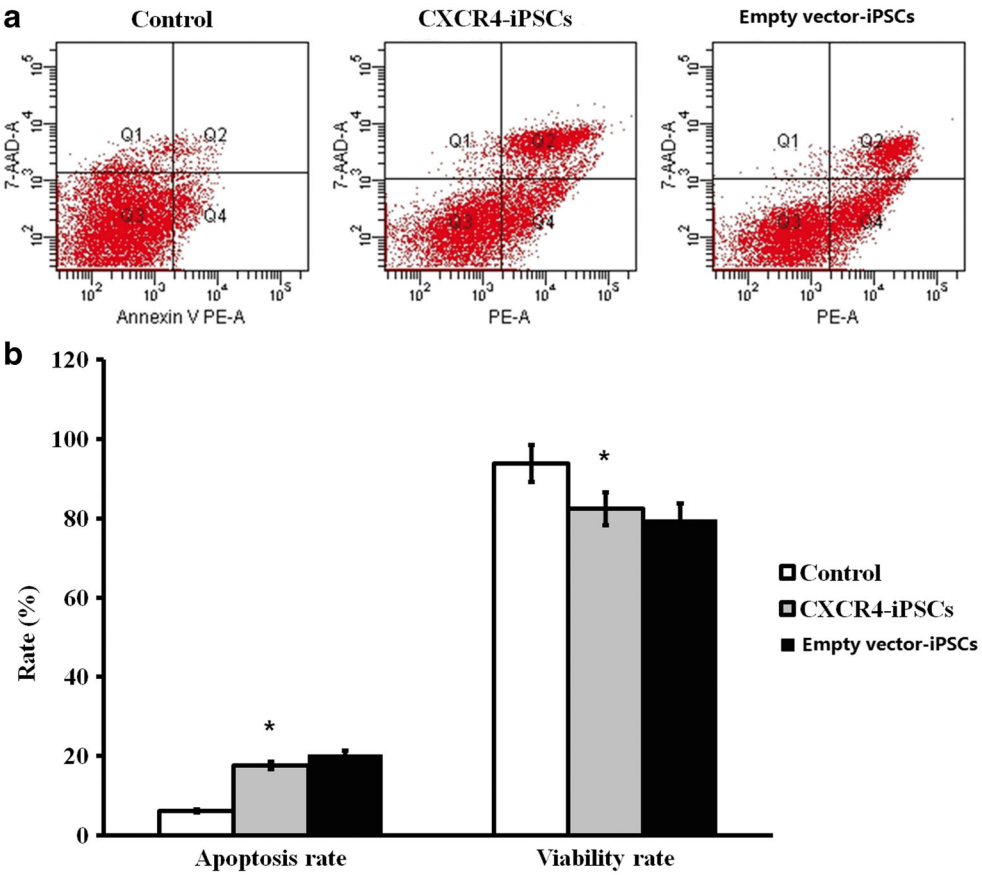

Fig. 5. The apoptosis of iPSCs after transfection. **a** Representative images of flow cytometric analysis of apoptosis (1×10^6/tube). **b** Histogram displayed the apoptosis and viability rate. ($n = 3$–4, one-way ANOVA, $*p < 0.05$ *vs* corresponding control).

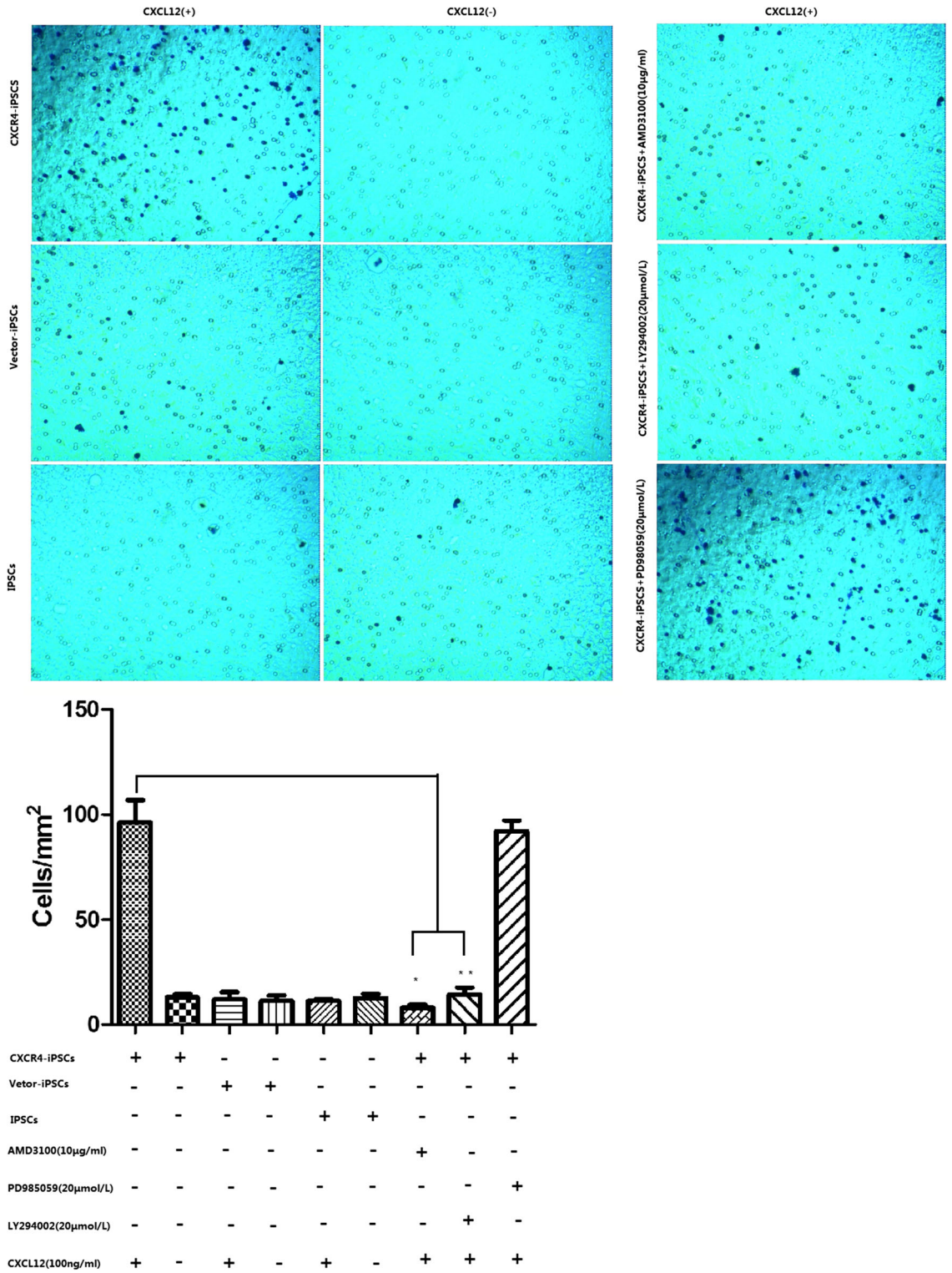

Fig. 6. Migration of the iPSCs. **a** Images of the transmigated iPSCs from the six representative groups (5×10^4/well). These iPSCs adhered to the lower surface of the cylonpore membrance in response to 100 ng/ml CXCL12 in transwell assay (magnification × 40). Scale bar 100 μm. **b** The comparison of the migration indexes among the eight groups. ($n = 3$–4, one-way ANOVA, $^*P < 0.05$, *vs.* the groups in response to the same concentration of CXCL12. The values represent the mean ± SD).

Effect of Lentiviral Infection and Upregulation of CXCR4 on Stemness of the Infected iPSCs

The expression levels of CXCR4 after transfection were significantly higher than the control group (Fig. 2a–g). Besides, demethylation status of a CpG island in the promoter region of CXCR4 gene as detected with the BSP method indicated a higher demethylation compared with the control group (Fig. 7i–j; $p < 0.05$). To evaluate if infection of iPSCs with CXCR4b-TAL-Tet1c lentiviral particle and the subsequently forced expression of endogenous CXCR4 alter the stemness of the iPSCs, the stem cell-like morphology after transfection is shown in Fig. 2b. Selected stem cell marker expression (Fig. 2c; $p > 0.05$), and CpG island in the promoter region of Oct4, c-Myc, Klf4, and Sox2 gene were also detected with BSP method (Fig. 7a–h); $p > 0.05$). The results suggest that CXCR4 did not alter demethylation status of a CpG island in the main promoter region of Oct4 and c-Myc genes, but a little transformation in Klf4 and Sox2.

Migration of the CXCR4-Expressing iPSCs

To investigate whether forced expression of CXCR4 enhances migration of the iPSCs toward the specific CXCR4 ligand CXCL12, the control and CXCR4-expressing iPSCs were cultured in transwell assembly. As evidenced with visualization of Trypan blue, the results show that exposure of the CXCR4-expressing iPSCs to CXCL12 for 4 h (260.8 ± 9.18) caused robust cell migration to the lower chamber supplemented with 100 ng/ml CXCL12 comparison to the control iPSCs (Fig. 6; $p < 0.05$). However, in the presence of AMD3100 for 1 h, a CXCR4 specific antagonist, the CXCR4-expressing iPSCs migrated little to the CXCL12-containing lower chamber as the control iPSCs (Fig. 6; $p > 0.05$), suggesting that at least portion of cell surface CXCR4 underwent internalization, and the antagonist inactivated the CXCR4 receptor.

There was no significant difference in the number of cell migration between iPSCs group, CXCR4-iPSCs group, and Vector-iPSCs group ($p > 0.05$). The migration of CXCR4-iPSCs + CXCL12 group was significantly higher than that iPSCs + CXCL12 group after exposure to CXCL12 for 4 h ($p < 0.05$), no significance in Vector-iPSCs + CXCL12 group. After pretreatment with CXCR4 receptor antagonist AMD3100, LY294002, and PD98059 for 1 h respectively, compared with CXCR4-iPSCs + CXCL12 group, AMD3100 and LY294002 significantly reduced cell migration ($p < 0.05$), but PD98059 had no significant effect on the migration of CXCR4-iPSCs ($p > 0.05$).

DISCUSSION

The emergence and development of iPSCs are considered as significant achievements in life and medical sciences [17]. Transplantation of iPSCs associates with significant increase of vascular density and reduces myocardial apoptosis in the border zone of infarction by mitigating the fibrosis [18]. Regardless the types and origin of stem cells used for cell transfer therapy, substantial cell death after transplantation into the ischemic or infracted heart has been a significant impediment to the efficacy [19]. Poor homing of the cells after transplantation is an unresolved common issue in cardiac cell therapies. CXCL12 are expressed in cardiac myocytes and fibroblasts. Its expression is significantly upregulated in MI [20–22], reaches peak by days 3 to 7, and maintains high for at least 14 days in the infracted area [23]. Besides the effect of enhancing angiogenesis, reducing myocytes apoptosis, increasing generation of new myocytes to enhance cardiac repair after experimental infarction [24], CXCL12/CXCR4 signaling activation increases cytosolic calcium transients in an IP3-denpendent manner and induces a positive chronotropic effect in a rat neonatal cardiomyocytes *in vitro* while it improves cardiac systolic function *in vivo* [25]. However, whether CXCL12 plays any cardioprotective roles through recruitment of iPSCs to the infracted area remains unclear.

The present study using a lentiviral vector system takes advantage of TALEs to improve the efficient activation of CXCR4 expression. Methylation of CpG dinucleotides is the major mechanism regulating mammalian gene expression [26], which seems a limitation for the use of conventional TALEs because promoter hypermethylation correlates with silencing of a significant fraction of genes [27]. TALENs having the hydroxylase catalytic domain of ten-eleven translocation 1 (TET1) as a functional domain catalyze the first step in the active demethylation of 5-methylcytisine, the oxidation of 5-methylacytosine to 5-hydroxymethlcytosine.

For CXCR4 target sites, we found that the chimeric TALEs bearing the TET1 catalytic domain induced significant expression of luciferase in both HEK293 cells and COS-1 cells (Fig. 1). However, we did not detect the degree and range of the actual CpG demethylation that

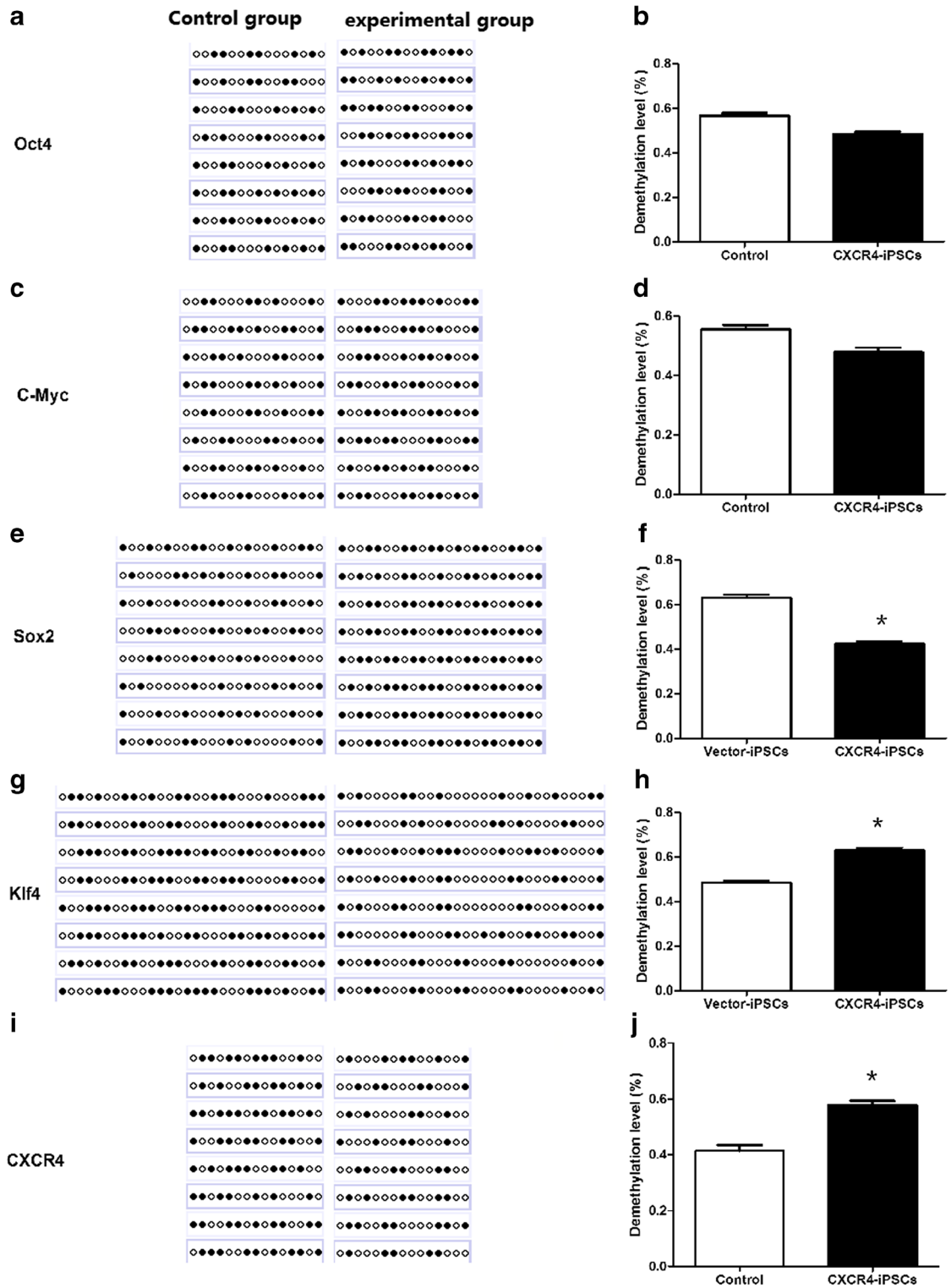

Fig. 7. CpG demethylation of the promoter regions of CXCR4 (**i**), Oct4 (**a**), Klf4 (**g**), Sox2 (**e**), and c-Myc (**c**) in iPSCs infected with CXCR4b-TAL-Tet1c. The average demethylation levels were calculated as the ratio of methylated CpG sites to all CpG sites tested. Histogram displayed CpG demethylation in **b**, **d**, **f**, **h,** and **j**. ($n = 8$, one-way ANOVA, $^*p < 0.05$ *vs* corresponding control).

was induced to the methylated promoter reporter in the transfected cells and the endogenous CXCR4 promoter region in the mouse iPSCs. Transient transfection and lentiviral transduction may result in differential degree and range in demethylation. Such discrepancy is due to sustained expression of CXCR4b-TAL-Tet1c in lentiviral-infected iPSCs. The evidence that transient transfection of CXCR4b-TAL-Tet1c plasmid in HEK293 cells and COS-1 cells induces significant expression of luciferase suggests that transient transfection of CXCR4b-TAL-Tet1c mRNA should also work well. In general, mRNA transfection generates much higher efficiency than plasmid DNA transfection does. This not only eliminates viral infection and the related side effects, but also avoids any unnecessarily sustained expression after the successful demethylation. Viral infection and unnecessarily sustained expression may become a pronounced problem later *in vivo*, particularly for the cardiomyocytes differentiated from the transplanted iPSCs. However, these concerns are beyond the scope of this manuscript and will be addressed in future experiments.

Increase of expression of CXCR4 in the iPSCs after transfection resulted in 3.9-fold improvement of cell migration *in vitro*. It was initiated by CpG demethylation approach, and previous results have shown consistently that loci-specific CpG methylation and demethylation generally cover a range of 300 bp on both directions from the site of targeting [11]. However, whether this degree of improvement in CXCR4 migration is sufficient for stem cell homing *in vivo*, if further increased expression of CXCR4 will further enhance the migration, if use of non-lentiviral vectors without host genome integration offers any advantage, and if further enhanced migration is necessary for appropriate process of repair and regeneration are questions awaiting for future *in vivo* experiments to address. It is technically possible to further increase the CXCR4 expression with introduction of additional co-activating factors such as EP300 (KAT3B), a H3K27 acetyltransferase [28].

Although the targeting sequences were carefully selected and bioinformatics query of mouse genome with the selected targeting sequences did not identify any possible off-target sites, it is by no means that possible off-target demethylation is ruled out. However, depending upon the exact location of off-target demethylation that occurs, the toxic effect can be neglected since methylation and demethylation at a transcription regulation-insensitive region will unlikely result in any change in gene transcription.

The finding in this paper suggests that the expression of CXCR4 enhances migration of the iPSCs toward the specific CXCR4 ligand CXCL12, and CXCL12 binds to CXCR4 initiates divergent signaling pathways downstream of ligand binding, which can result in a variety of responses such as AKT and ERK1/2 [29, 30]. CXCL12 has been shown to guide neuron migration, pathogenic inflammation, as well as cardiogenesis [31–33]. The precise nature of these pathways may be tissue-dependent and thus may differ between cell types. In this regard, similar signaling molecules seem to play a different regulatory role downstream of CXCR4 and CXCL12. CXCR4 enhanced the migration of iPSCs by activating the AKT, which were blocked by AMD3100. However, which signaling was associated with ERK1/2 after CXCL12 bound to CXCR4 in iPSCs calls for further studies.

A crucial hurdle for therapeutic application of iPSCs is their potential to form tumors *in vivo*, but the residual risk for teratoma of CXCR4-iPSCs is unknown since CXCR4 altered demethylation status of Klf4 and Sox2 gene. This deserves further investigation.

In summary, loci-specific CpG demethylation of CXCR4 promoter region with TALE-Tet1c successfully activated the expression of CXCR4 in mouse iPSCs. This proof-of-concept study has paved the way for future *in vivo* experiments in rodent models of MI and heart failure.

AUTHORS' CONTRIBUTIONS

CJ conducted the most of the experiments and wrote the paper. JG conceived the idea for the paper, conducted experiments of real-time PCR and cell viability, and wrote the paper with CJ; and HYC conducted experiments on the CXCR4 reporter construction and *in vitro* CpG methylation. YHF revised the paper critically for important intellectual content, analyzed the experiments of Figs. 1 and 2, final approvaled of the version to be published.

FUNDING

This work was supported in part by the National Natural Science Foundation of China [81673635 and 81100078], Scientific research project of Guangdong Provincial Administration of traditional Chinese Medicine [20171072], and Science Research Foundation of Jinan university [21615478].

COMPLIANCE WITH ETHICAL STANDARDS

Competing Interests. The authors declare that they have no competing interests.

REFERENCES

1. Lunde, K., and S. Aakhus. 2008. Cell therapy in acute myocardial infarction: measures of efficacy. *Heart* 94: 969–970.
2. Yang, L., M.H. Soonpaa, E.D. Adler, T.K. Roepke, S.J. Kattman, M. Kennedy, E. Henckaerts, K. Bonham, G.W. Abbott, R.M. Linden, L.J. Field, and G.M. Keller. 2008. Human cardiovascular progenitor cells develop from a KDR+ embryonic-stem-cell-derived population. *Nature* 453: 524–528.
3. Martins, A.M., G. Vunjak-Novakovic, and R.L. Reis. 2014. The current status of iPS cells in cardiac research and their potential for tissue engineering and regenerative medicine. *Stem Cell Reviews* 10: 177–190.
4. Gersbach, C.A., T. Gaj, and C.F. Barbas III. 2014. Synthetic zinc finger proteins: the advent of targeted gene regulation and genome modification technologies. *Accounts of Chemical Research* 47: 2309–2318.
5. Sander, J.D., and J.K. Joung. 2014. CRISPR-Cas systems for editing, regulating and targeting genomes. *Nature Biotechnology* 32: 347–355.
6. Reyon, D., S.Q. Tsai, C. Khayter, J.A. Foden, J.D. Sander, and J.K. Joung. 2012. FLASH assembly of TALENs for high-throughput genome editing. *Nature Biotechnology* 30: 460–465.
7. Pattanayak, V., S. Lin, J.P. Guilinger, E. Ma, J.A. Doudna, and D.R. Liu. 2013. High-throughput profiling of off-target DNA cleavage reveals RNA-programmed Cas9 nuclease specificity. *Nature Biotechnology* 31: 839–843.
8. Ebina, H., Y. Kanemura, N. Misawa, T. Sakuma, T. Kobayashi, T. Yamamoto, and Y. Koyanagi. 2015. A high excision potential of TALENs for integrated DNA of HIV-based lentiviral vector. *PLoS One* 10: e0120047.
9. Mussolino, C., R. Morbitzer, F. Lutge, N. Dannemann, T. Lahaye, and T. Cathomen. 2011. A novel TALE nuclease scaffold enables high genome editing activity in combination with low toxicity. *Nucleic Acids Research* 39: 9283–9293.
10. Maeder, M.L., J.F. Angstman, M.E. Richardson, S.J. Linder, V.M. Cascio, S.Q. Tsai, Q.H. Ho, J.D. Sander, D. Reyon, B.E. Bernstein, J.F. Costello, M.F. Wilkinson, and J.K. Joung. 2013. Targeted DNA demethylation and activation of endogenous genes using programmable TALE-TET1 fusion proteins. *Nature Biotechnology* 31: 1137–1142.
11. Li, K., J. Pang, H.Y. Cheng, W.P. Liu, J.M. Di, H.J. Xiao, Y. Luo, H. Zhang, W.T. Huang, M.K. Chen, L.Y. Li, C.K. Shao, Y.H. Feng, and X. Gao. 2015. Manipulation of prostate cancer metastasis by locus-specific modification of the CRMP4 promoter region using chimeric TALE DNA methyltransferase and demethylase. *Oncotarget* 6: 10030–10044.
12. Cencioni, C., M.C. Capogrossi, and M. Napolitano. 2012. The SDF-1/CXCR4 axis in stem cell preconditioning. *Cardiovascular Research* 94: 400–407.
13. Wu, Y., and R.C. Zhao. 2012. The role of chemokines in mesenchymal stem cell homing to myocardium. *Stem Cell Reviews* 8: 243–250.
14. Tang, Y.L., W. Zhu, M. Cheng, L. Chen, J. Zhang, T. Sun, R. Kishore, M.I. Phillips, D.W. Losordo, and G. Qin. 2009. Hypoxic preconditioning enhances the benefit of cardiac progenitor cell therapy for treatment of myocardial infarction by inducing CXCR4 expression. *Circulation Research* 104: 1209–1216.
15. Askari, A.T., S. Unzek, Z.B. Popovic, C.K. Goldman, F. Forudi, M. Kiedrowski, A. Rovner, S.G. Ellis, J.D. Thomas, P.E. DiCorleto, E.J. Topol, and M.S. Penn. 2003. Effect of stromal-cell-derived factor 1 on stem-cell homing and tissue regeneration in ischaemic cardiomyopathy. *Lancet* 362: 697–703.
16. Jiang, J., W. Lv, X. Ye, L. Wang, M. Zhang, H. Yang, M. Okuka, C. Zhou, X. Zhang, L. Liu, and J. Li. 2013. Zscan4 promotes genomic stability during reprogramming and dramatically improves the quality of iPS cells as demonstrated by tetraploid complementation. *Cell Research* 23 (1): 92–106.
17. Yamanaka, S. 2007. Strategies and new developments in the generation of patient-specific pluripotent stem cells. *Cell Stem Cell* 1: 39–49.
18. Song, G., X. Li, Y. Shen, L. Qian, X. Kong, M. Chen, K. Cao, and F. Zhang. 2015. Transplantation of iPSc restores cardiac function by promoting angiogenesis and ameliorating cardiac remodeling in a post-infarcted swine model. *Cell Biochemistry and Biophysics* 71: 1463–1473.
19. Menasche, P. 2004. Cellular transplantation: hurdles remaining before widespread clinical use. *Current Opinion in Cardiology* 19: 154–161.
20. Pillarisetti, K., and S.K. Gupta. 2001. Cloning and relative expression analysis of rat stromal cell derived factor-1 (SDF-1)(1): SDF-1 alpha mRNA is selectively induced in rat model of myocardial infarction. *Inflammation* 25: 293–300.
21. Takahashi, M. 2010. Role of the SDF-1/CXCR4 system in myocardial infarction. *Circulation Journal* 74: 418–423.
22. Hu, X., S. Dai, W.J. Wu, W. Tan, X. Zhu, J. Mu, Y. Guo, R. Bolli, and G. Rokosh. 2007. Stromal cell derived factor-1 alpha confers protection against myocardial ischemia/reperfusion injury: role of the cardiac stromal cell derived factor-1 alpha CXCR4 axis. *Circulation* 116: 654–663.
23. Yu, J., M.C. Li, Z.L. Qu, D. Yan, D. Li, and Q.R. Ruan. 2010. SDF-1/CXCR4-mediated migration of transplanted bone marrow stromal cells toward areas of heart myocardial infarction through activation of PI3K/Akt. *Journal of Cardiovascular Pharmacology* 55: 496–505.
24. Tilokee, E.L., N. Latham, R. Jackson, A.E. Mayfield, B. Ye, S. Mount, B.K. Lam, E.J. Suuronen, M. Ruel, D.J. Stewart, and D.R. Davis. 2016. Paracrine engineering of human explant-derived cardiac stem cells to over-express stromal-cell derived factor 1alpha enhances myocardial repair. *Stem Cells* 34: 1826–1835.
25. Hadad, I. 2013. Stroma cell-derived Factor-1 alpha signaling enhances calcium transients and beating frequency in rat neonatal cardiomyocytes. *PLoS One* 8: e56007.
26. Suzuki, M.M., and A. Bird. 2008. DNA methylation landscapes: provocative insights from epigenomics. *Nature Reviews. Genetics* 9: 465–476.
27. Deng, D., P. Yin, C. Yan, X. Pan, X. Gong, S. Qi, T. Xie, M. Mahfouz, J.K. Zhu, N. Yan, and Y. Shi. 2012. Recognition of methylated DNA by TAL effectors. *Cell Research* 22: 1502–1504.

28. Tang, Z., W.Y. Chen, M. Shimada, Kim J. Nquyen, X.J. Sun, T. Senqoku, R.K. McGinty, J.P. Fernandez, T.W. Muir, and R.G. Roeder. 2013. SET1 and p300 act synergistically, through coupled histone modifications, in transcriptional activation by p53. *Cell* 154: 297–310.
29. Delgado-Martin, C., C. Escribano, J.L. Pablos, L. Riol-Blanco, and J.L. Rodriguez-Fernandez. 2011. Chemokine CXCL12 uses CXCR4 and a signaling core formed by bifunctional Akt, extracellular signal-regulated kinase (ERK)1/2, and mammalian target of rapamycin complex 1 (mTORC1) proteins to control chemotaxis and survival simultaneously in mature dendritic cells. *The Journal of Biological Chemistry* 286: 37222–37236.
30. Yang, F., W. Sun, Y. Yang, C.L. Li, H. Fu, X.L. Wang, F. Yang, T. He, and J. Chen. 2015. SDF1-CXCR4 signaling contributes to persistent pain and hypersensitivity via regulating excitability of primary nociceptive neurons: involvement of ERK-dependent Nav1.8 up-regulation. *Journal of Neuroinflammation* 12: 219.
31. Ryu, C.H., S.A. Park, S.M. Kim, J.Y. Lim, C.H. Jeong, J.A. Jun, J.H. Oh, S.H. Park, W.I. Oh, and S.S. Jeun. 2010. Migration of human umbilical cord blood mesenchymal stem cells mediated by stromal cell-derived factor-1/CXCR4 axis via Akt, ERK, and p38 signal transduction pathways. *Biochemical and Biophysical Research Communications* 398: 105–110.
32. Zilkha-Falb, R., N. Kaushansky, N. Kawakami, and A. Ben-Nun. 2016. Post-CNS-inflammation expression of CXCL12 promotes the endogenous myelin/neuronal repair capacity following spontaneous recovery from multiple sclerosis-like disease. *Journal of Neuroinflammation* 13: 7.
33. Zou, Y.R., A.H. Kottmann, M. Kuroda, I. Taniuchi, and D.R. Littman. 1998. Function of the chemokine receptor CXCR4 in haematopoiesis and in cerebellar development. *Nature* 393: 595–599.